Journal of Imaging Science and Technology® 51(1): 34–43, 2007.

High Dynamic Range Image Compression by Fast Integrated Surround Retinex Model

Lijie Wang, Takahiko Horiuchi and Hiroaki Kotera
Graduate School of Science and Technology, Chiba University, Inage-ku, Chiba, Japan
E-mail: lijiewang@graduate.chiba-u.jp

Abstract. *A novel compressing method of high dynamic range image based on fast integrated surround Retinex model is proposed in this paper. The proposed method has two novelties. First, multiscale surround images are integrated to a single surround field, which is applied to center/surround single-scale Retinex (SSR) model. The method reduces the "banding artifact" seen in normal SSR and simplifies the complicated computational steps in conventional multiscale Retinex. Second, the Gaussian pyramid method is introduced to cut the computation time for generating a large-scale surround by tracing a "reduction" and "expansion" sequences using down and up sampling followed by linear interpolation. The computational expense is dramatically saved less than 1/100 for getting a surround by Gaussian convolution with large kernel size. The proposed model worked well in compressing the dynamic range and improving the visibility in heavy shadow areas of natural color images while preserving pleasing contrast.*

[DOI: 10.2352/J.ImagingSci.Technol.(2007)51:1(34)]

INTRODUCTION

Human vision is a complicated automatic self-adaptation system. It is capable of seeing over five orders in magnitude simultaneously and can gradually adapt to scenes with high dynamic ranges of over nine orders in magnitude. The current display devices, such as cathode ray tube (CRT), cannot capture the dynamic range more than 100:1. To recreate the viewer's sensation of the original scene in current display devices, the high dynamic range (HDR) of the scene has to be compressed to the low dynamic range of the device. This is a difficult problem because the visual system is too complicated and current technique cannot yet understand it completely.

The many published papers on HDR image compression are classified into two groups: *Spatially-invariant* tone reproduction curve (TRC) and *spatially-variant* tone reproduction operator (TRO) methods.[1] TRC operates pointwise on the image data which is actually based on the global adaptation of human vision. Algorithms by Tumblin et al.,[2] Tumblin and Rushmeier,[3] belong to this catagory. Pattanaik et al.[4] proposed a time-dependent method based on the time adaptation of human vision, which also uses the global adaptation models. TRO uses the spatial structure of the image data and attempts to preserve local image contrast. The algorithm by Chiu et al.[5] belongs to this catagory. TRC is simple and efficient, but at the expense of local contrast loss because of processing the whole image with a single curve. TRO, which is traditionally based on a multiresolution decomposition algorithm, such as Gaussian decomposition, works well in measuring and preserving local image contrast. However, any methods can model only a part of the complicated adaptation process of human vision.

This paper follows the method of TRO, but presents a new idea based on the Retinex theory of the human vision process. Retinex is a typical method of TRO and has been broadly used in image processing, such as color image appearance improvement,[6,7] and also HDR image compression, e.g., by Carrato[8] who adopts a rational filter substituting for a Gaussian filter. Human vision can see the world without being affected by the spatially nonuniformity of illumination and the color of the illuminant, with what we call lightness and color constancies. Based on these characteristics, Land and McCann proposed Retinex.[9–14] Retinex is very useful in color image processing and has been improved during past forty years. Multiscale Retinex (MSR), generated by the weighted sum of multiple single-scale Retinex (SSR), is the most popular algorithm, because it can suppress the banding artifacts around high contrast edges in SSR. Since the optimization of weights is not easy,[15] conventional MSR simply applies equal weights to all scales of SSR but does not always give a satisfactory image. Kotera et al.[6,7] proposed an adaptive scale-gain MSR to improve the color appearance in conventional MSR, but the selection of scales and weights is still complicated, and the computation cost is too expensive.

In this paper, a new fast and simple algorithm is proposed without banding artifacts caused by the conventional SSR model. The proposed algorithm adopts an integrated multiscale surround image composed of several luminance surround images to apply to the SSR model, which substitutes for the conventional integrated MSR composed of several SSR. The Gaussian pyramid is introduced to generate an integrated surround image quickly. The original image is repeatedly down sampled and divided by 2 in width and height, and the coarsest down-sampled image on the top of the pyramid is convoluted with the corresponding smallest size Gaussian filter, resulting in a surround image equivalent to the largest kernel size, so that the computational expense is dramatically reduced. By this model we get results comparable to the published papers in HDR image compression.

In the following sections, first, we review the recent

Received Sep. 12, 2005; accepted for publication Jun. 6, 2006.
1062-3701/2007/51(1)/34/10/$20.00.

progress in Retinex models. Next we propose the integrated surround Retinex algorithm, and third discuss the optimum parameters and improvement in speed. In addition, HDR image compression gives some examples which demonstrate good visibility in heavy shadow while preserving pleasing local contrast. Finally, we draw conclusions and insight into our future work.

RETINEX MODEL

The Retinex algorithm proposed by Land[9–13] is based on their Mondrian experiments and was improved by McCann et al.[16] It is a classical vision model with forty years history and recently received attention again.[17] Land suggested that color appearance is controlled by surface reflectance rather than by the distribution of reflected light and proposed three color mechanisms for the spectral responses of the cone photoreceptors. He called these mechanisms Retinexes because they are thought to be some combination of retinal and cortical mechanisms.[18]

According to Land, human visual system has the functions that recognize the world without being affected by spatially nonuniform distribution of illuminant. Basically Retinex is a model that eliminates the effect of the nonuniformity of illumination. Simply, the image I captured by camera is equivalent to the product of the reflectance R and illuminant distribution L. According to $R \cong I/L$, we can restore reflectance R from Image I by inferring illumination L.

Though various enhancements to the theory have been proposed, its key feature is that the Retinex algorithm explicitly treats the spatial distribution of illumination. According to the path-based model based on Mondrian experiments of Land and McCann,[10] the luminance difference of two separated points in the scene is obtained by the ratio of the neighboring points along the path. When gray step patches with linear reflectance are lit by the illumination which has the opposite gradient, the sequence of darkness appearance is not changed regardless of whether each patch reflects the same amount of light physically, if the relative luminance ratios on the boundaries of each edge are traced. To estimate the distribution of illumination L, various ways of taking paths into account have been published. The random walk model[18] computes the luminance product of each point from the distributed initial points in the image by a random walk. The Poisson model[19] approaches the spatial gradient in illumination from the change in the second derivative of the signal and computes it by inversion. McCann-Sobel model[20] iteratively computes the luminance ratio along spiral paths while continuing to down-sample the image. Another iterative model by Funt[21] traces eight neighbors. The iterative model is a two-dimensional extension of the path-based model, where a new value is calculated for each pixel by iterative comparison.

The center/surround model simply estimates the luminance L around a pixel in consideration by averaging the image I with Gaussian filter. Based on the work by Land,[13] NASA (Refs. 22–26) developed MSR model by integrating multiple SSRs with different scales and weights. Furthermore, a quadratic programming method minimizes a second differential cost function by determining undefined Euler-Lagrange coefficients under the constraint of a spatial smoothing condition for image and illumination. Because the path-based model is complicated, the concise center/surround model is selected in this paper. The reflectance image $R(x,y)$ is calculated by the ratio of center $I(x,y)$ to the surround $S(x,y)$, simply noted as $R=C/S$. The spatial distribution of illumination $L(x,y)$ is equivalent to surround, which is calculated by averaging the original image $I(x,y)$ with a Gaussian filter.

The most representative C/S MSR model of NASA is processed in logarithmic space. The following equations describe the process:

$$R^i_{\mathrm{MSR}}(x,y) = \sum_{m=1}^{M} w_m R^i_{\mathrm{SSR}}(x,y,\sigma_m);\ i = R,G,B, \tag{1}$$

$$R^i_{\mathrm{SSR}}(x,y,\sigma_m) = \log \frac{I_i(x,y)}{I_i(x,y) \otimes G_m(x,y)};\ i = R,G,B, \tag{2}$$

$$G_m(x,y) = K_m \exp\{-(x^2+y^2)/\sigma_m^2\}, \quad \int\int G_m(x,y)\,dx\,dy = 1. \tag{3}$$

Equation (2) expresses the output of SSR model as the ratio of the center pixel $C=I_i(x,y)$ to the surround $S=I_i \otimes G_m$, where G_m denotes Gaussian averaging filter with scale m and standard deviation σ_m and the symbol $\otimes$ denotes convolution. The defect of SSR is a banding artifact appears around high contrast edges. A MSR model without banding artifact has been developed by Jobson et al.,[22–26] integrating multiple SSRs with different standard deviations σ_m and appropriate weight w_m as expressed by Eq. (1). However, the optimization process of σ_m and w_m is unclear and these parameters must be decided by trial and error. In addition, logarithmic conversion accentuates the dark noise level in shadow region and the dynamic range expansion in the processed image needs to be limited. Furthermore, because the basic logarithmic model treats R, G, and B channels independently and the dynamic range of each channel is normalized to the range of the display device, the color balance cannot be maintained so that a wide uniform area in the image, such as sky or wall tends to a gray world. Jobson et al.[25] regulated the range of the output image by lower and upper clipping of the wide histogram. Rahman et al.[26] improved the color restoration with additional logarithmic terms corresponding to each color band signal divided by the sum of color band signals. They call this model multiscale Retinex with color restoration. Kotera et al.,[6] proposed an adaptive scale-gain MSR model with stable and excellent color reproduction in linear space without using logarithmic conversion. In this model, the surround image generated only from the luminance image is used for the R, G, and B channels in common, which maintains the color balance. They also proposed an automatic setting method for weights adapted to the scale

gain. However, since the computation for weights needs the histograms luminance SSRs corresponding to the multiple scales and takes too much time with increasing Gaussian kernel size, it still needs improvement for practical use.

INTEGRATED-SURROUND RETINEX MODEL

In this paper, we propose a concise new Retinex model different from the conventional MSR. Our work is mainly based on the work of Kotera et al.[6,7] First, we adopted linear space without logarithmic conversion to avoid instability for noise and output range spreading in dark shadows. Second, we used only the luminance channel to form the surround for each color channel in order to keep color balance. The major difference from Kotera's method is that the new model creates an integrated multiscale luminance surround from multiple luminance surround images by Gaussian filters with different standard deviation σ_m. The proposed model can suppress unwanted banding artifacts as well as the adaptive MSR model of Kotera. We introduced the Gaussian pyramid to produce the integrated surround image, by which the convolution computation for smoothing the original image with a Gaussian filter was dramatically reduced. The following subsection details improvements in our new algorithm.

Integrated-Surround Retinex Algorithm

Figure 1 illustrates the proposed integrated-surround Retinex model. Instead of the weighting sum of multiple SSRs, the proposed model integrates $m=1\sim M$ different surround images S_m into a single surround image S_{sum} with adaptive weight parameters $w(\sigma_m)$. To keep color balance, S_m is calculated by convoluting the luminance image $Y(x,y)$ with the Gaussian filter G_m with standard diviation σ_m as Eq. (6) expressed. The output of Eq. (4) is the ratio of the center pixel I_i to integrated luminance surround S_{sum} and A is a gain coefficient which will be discussed detailed in the coming section on optimum parameters

$$\text{SSR}_{\text{sum}}(x,y,\sigma_m) = A\frac{I_i(x,y)}{S_{\text{sum}}(x,y,\sigma_m)};$$
$$i=\text{R,G,B},A\text{: gain coefficient}, \quad (4)$$

$$S_{\text{sum}}(x,y,\sigma_m) = \sum_{m=1}^{M} w(\sigma_m)S_m(x,y,\sigma_m), \quad (5)$$

$$S_m(x,y,\sigma_m) = \langle G_m(x,y) \otimes Y(x,y)\rangle;$$
$$\sigma_m = 2^m,\ Y(x,y)\text{: luminance channel}, \quad (6)$$

where

$$\sum_{m=1}^{M} w(\sigma_m) = 1. \quad (7)$$

In the proposed method, M times of division is avoided in the computation of multiple SSRs and replaced with the easy summation instead. Figure 2(f) shows a sample obtained from the SSR process by the proposed method by integrating the three surround images of $\sigma_m=(8,32,128)$ with uniform weight of 1/3. It does not provide the dramatic improvement in shadow appearance as does NASA as shown in Fig. 2(d) or our previous adaptive scale-gain MSR in Fig. 2(e), but it suppresses the banding artifact very well in comparison with a conventional middle scale SSR in Fig. 2(b) and is clearly better than the large scale SSR in Fig. 2(c). In addition, contrast appears more natural without over emphasis in comparison with NASA in Fig. 2(d) or our previous MSR in Fig. 2(e).

Optimum Parameters

The Retinex model aims to reproduce the original visual images, but in practice, the original scene is usually unknown unless the observer has seen the captured scene standing at the same place and the same time. Thus the setting of the optimum parameters is difficult without the original image. In this paper, as illustrated in Fig. 3, a test scene "color block" under nonuniform illumination in our laboratory is captured by a digital camera, then the camera image is modified using Adobe Photoshop™ by trial and error method until it is seen approximately matched to the visual scene. The modified image is taken as a target image.[7]

To make a quantitative estimation for the proposed model and find the optimum parameters, the color differences ΔE^*_{ab} between the visual target image and the processed images are evaluated in CIELAB color space as follows:

$$\Delta E^*_{ab} = (\Delta L^{*2} + \Delta a^{*2} + \Delta b^{*2})^{1/2}, \quad (8)$$

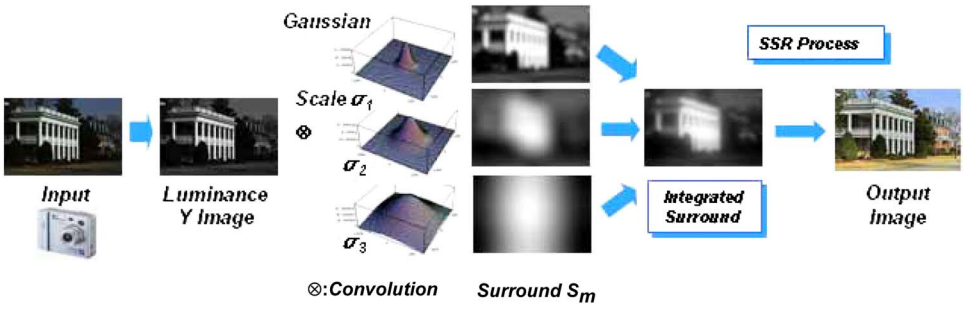

Figure 1. Proposed Retinex model using integrated surround.

$$\Delta L^* = L_R^* - L_V^*, \quad \Delta a^* = a_R^* - a_V^*, \quad \Delta b^* = b_R^* - b_V^*, \quad (9)$$

where L^*, a^*, and b^* are tristimulus values of CIELAB color space, R represents the results of proposed method, V represents target image

$$L^* = 116 * f\left(\frac{Y}{Y_n}\right) - 16,$$

$$a^* = 500 * \left\{ f\left(\frac{X}{X_n}\right) - f\left(\frac{Y}{Y_n}\right) \right\},$$

$$b^* = 200 * \left\{ f\left(\frac{Y}{Y_n}\right) - f\left(\frac{Z}{Z_n}\right) \right\},$$

$$f(t) = \begin{cases} t^{1/3} & for\ t > 0.008856 \\ 7.787t + 16/116 & for\ t \leqslant 0.008856, \end{cases} \quad (10)$$

where X, Y, and Z are CIEXYZ tristimulus values and X_n, Y_n, and Z_n are the CIEXYZ tristimulus values of the reference white point. Considering the computation expense and processing speed, it is hoped to produce a MSR image from a small number of SSRs. Empirically, to produce a MSR image without banding artifact, at least three SSR images are needed. As well, first, we used three scales ($M=3$) of surround images, small ($\sigma_1=2$), middle ($\sigma_2=16$), and large ($\sigma_3=128$) to get an integrated surround in the proposed method. Then we adjusted the weights $w(\sigma_m)$ to minimize the color difference between the target image C and the processed output for the camera image B in Fig. 3. Figure 4 illustrates the results in the case of $M=3$. Because the possible number of combinations for the weights $w(\sigma_m)$ with gain parameter A becomes too large, we cut the unnecessary tests by observing the tendency of color difference changes corresponding to each combination. First fixing the weight $w(\sigma_1)$ to 0.1, with the condition $w(\sigma_1)+w(\sigma_2)+w(\sigma_3)=1$, a combination of $w(\sigma_2)$ and $w(\sigma_3)$ is changed. Next fixing $w(\sigma_2)$ to 0.1, a combination of $w(\sigma_1)$ and $w(\sigma_3)$ is also changed. When the gain $A=0.8$ and the weights $w(\sigma_1)=0.3$, $w(\sigma_2)=0.1$, and $w(\sigma_3)=0.6$, the smallest color difference $\Delta E_{ab}^*=8.6$ is obtained. From the tendency of these color difference changes in Fig. 4, we can draw the conclusion that with the decrease in $w(\sigma_3)$, the smallest color difference corresponding to each combination tends to increase and goes

Figure 2. Sample by proposed Retinex model in comparison with conventional methods.

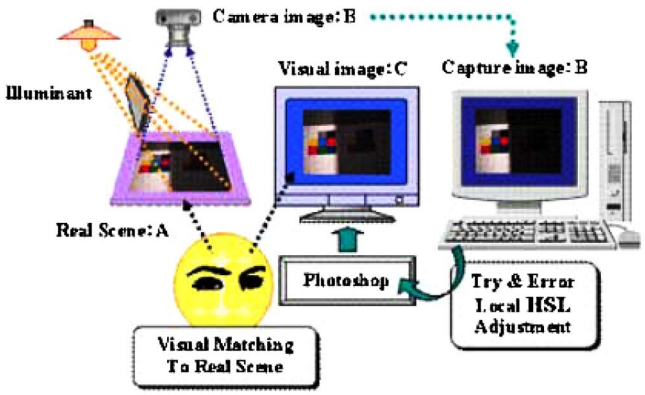

Figure 3. Synthesis of target image visually matched to real scene.

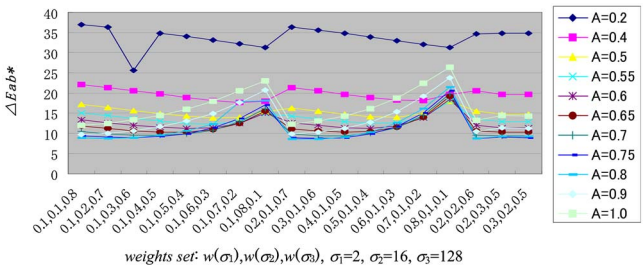

Figure 4. Color reproducibility by proposed model with three-scale sets ($\sigma_m=2, 16, 128$).

up rapidly for $w(\sigma_3)<0.5$. Hence $w(\sigma_3)\geqq 0.5$ and large scale $\sigma_3=128$ are necessary. We verified this condition again by fixing $w(\sigma_3)$ to 0.6 and 0.5, respectively, while changing a combination of $w(\sigma_1)$ and $w(\sigma_2)$, and reached the same conclusion, which is almost the same as reported by Yoda et al.[7]

We can also draw another conclusion from the experiments, namely that $w(\sigma_1)$ is more important than $w(\sigma_2)$ in color reproduction, because the smallest color difference increased for $w(\sigma_2)>w(\sigma_1)$ when $w(\sigma_3)$ is fixed to around 0.5. Thus we moved to the tests for the simpler case of two scales where the middle scale $\sigma_2=16$ is discarded and a combination of small ($\sigma_1=2$) and large ($\sigma_3=128$) scales are used. The same test process is performed. Figure 5 illustrates the results in the case of $M=2$. When the gain: $A=0.8$, and weights: $w(\sigma_1)=0.4$, $w(\sigma_3)=0.6$, the best result $\Delta E^*_{ab}=8.54$ is obtained, which is a little bit smaller than the case of three scales ($M=3$), but considered to be almost the same color reproducibility as the result with three surround images.

In addition, we also tested the color reproducibility for a different set of three scales ($\sigma_1=8$, $\sigma_2=32$, $\sigma_3=128$). As illustrated in Fig. 6, the minimum color difference ΔE^*_{ab} is obtained when the gain $A=0.8$ and weights $w(\sigma_1)=0.2$, $w(\sigma_2)=0.1$, and $w(\sigma_3)=0.7$, but it is a little bit worse than shown in Fig. 4 ($M=3$) and Fig. 5 ($M=2$).

The typical resultant images are compared with NASA (d) and our previous adaptive scale-gain MSR (h) in Fig. 7. The best image with the smallest color difference for $M=3$ by the proposed model is shown in Fig. 7(e) and that for $M=2$ in Fig. 7(f), respectively. In a tested color block image, banding artifacts are not seen in the reproduction by the proposed integrated-surround Retinex model using only two scales of luminance surround images.

Improvement in Fast Computation

The Retinex algorithm is very time-intensive due to a convolution between the original image and Gaussian filters in order to calculate surround images. Particularly, as the kernel size of the Gaussian filter increases, the computation time dramatically increases. The proposed model has the same problem, too. For example, when using a Gaussian filter with $\sigma=128$ (kernel size$=4\sigma+1=513\times513$ pixels) for the image size 1280×960, it took more than one hour (Pentium 1 GHz, Memory 256 MB, MATLAB). For practical use, the time expense has to be reduced. Because time is mainly consumed in calculating the surround image, the Gaussian pyramid method is introduced to accelerate the

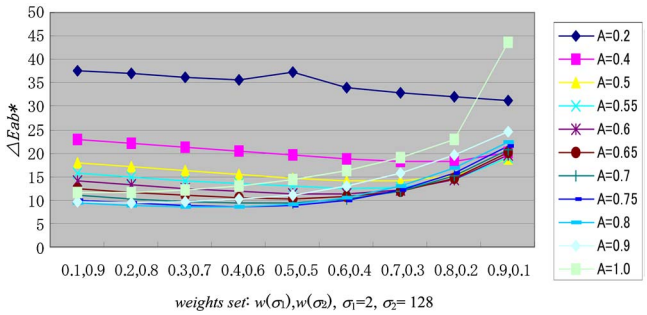

Figure 5. Color reproducibility by proposed model with two-scale sets ($\sigma_m=2,128$).

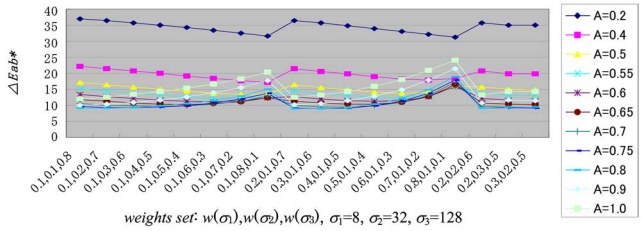

Figure 6. Color reproducibility by proposed model with three-scale sets ($\sigma_m=8,32,128$).

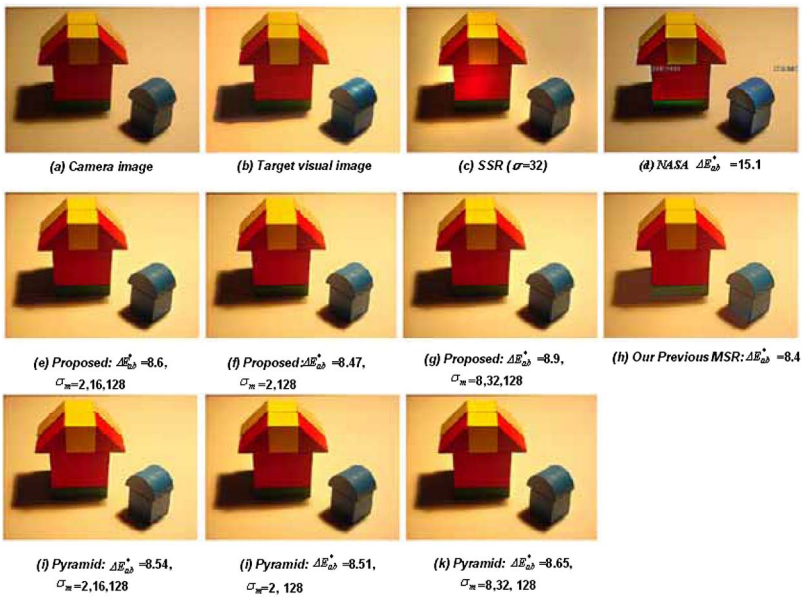

Figure 7. Color reproducibility results by the proposed model in comparison with conventional methods.

convolution speed in this paper. The Gaussian pyramid substitutes a large-scale convolution for a very small-scale one through up/down-sampling and interpolation sequences. Accordingly, the time expense is dramatically reduced.

The convolution process in Gaussian pyramid is illustrated in Fig. 8. First, the original luminance image $g_0(x,y)$ is placed at the bottom, and each successive higher level is a smaller version scaled down by 1/2 in width and height of the previous level. Through the K step sequences, image group: $g_1, g_2, \ldots, g_K$ is constructed. The image in level k is a copy reduced in resolution by 2^{-k} of the image $g_0(x,y)$ in level 0, which characterizes the multiresolution pyramid structure. The up process from g_0 to $g_1, \ldots, g_K$ is finished by down-sampling the low-pass image by a Gaussian filter with half the rate.

In this paper, we used a low pass filter with coefficients $w=[0.0500\ 0.2500\ 0.4000\ 0.2500\ 0.0500]$ approximated to Gaussian, which is circularly symmetric without half-pixel offsets. It works very rapidly because it is symmetric and applied separately in the horizontal and vertical directions.[2] Designating the 1/2 reduction function as Reduce, we express the upward down-sampling Gaussian pyramid by Eq. (11),

$$g_k = \text{Reduce}(g_{k-1}) = \text{Downsample}_{1/2}\{\text{Lowpass}(g_{k-1})\}$$

$$\text{Lowpass}(g_{k-1}) = \boldsymbol{m} \otimes g_{k-1};\ \otimes \text{ means convolution.}$$

$$\boldsymbol{m} = [m_{ij}] = [w_i \cdot w_j];\ i,j = 1,2, \ldots, 5$$

$$\boldsymbol{w} = [w_i] = [0.05, 0.25, .\ 0.4, .\ 0.25, .\ 0.05]:$$

$$\text{lowpass filter coefficients.} \qquad (11)$$

When the reduced image g_k at the required level K is obtained, convolution with a small-sized Gaussian filter with standard deviation σ_K creates the reduced surround image S_K corresponding to level K. Then S_K is expanded to twice in width and height by interpolation and up sampled at twice the rate. The process is repeated until the surround image S_0 with the same size as the original image is obtained. This downward up-sampling process is expressed by Eqs. (12) and (13),

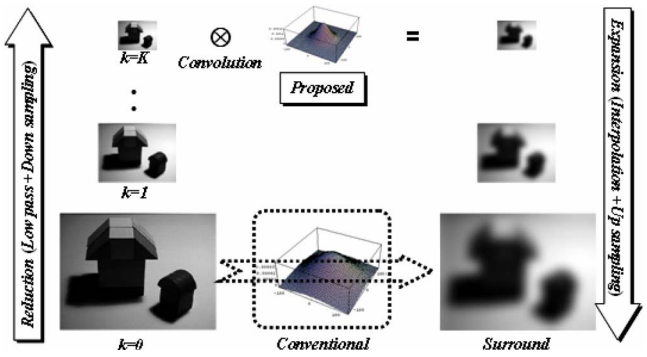

Figure 8. Fast computation method for surround by Gaussian pyramid.

$$S_K = g_K \otimes G_m(x,y,\sigma_K), \qquad (12)$$

$$S_{k-1} = \text{Expand}(s_k) = \text{Upsample}_2\{\text{Interpolate}(s_k)\};$$
$$k = K, K-1, \ldots, 1. \qquad (13)$$

The surround S_m expressed in Eq. (6) can be substituted by S_0, and according to the Gaussian pyramid, S_0 can be obtained by the K-step up-sampling process after convoluting g_K with the Gaussian filter $G_m(\sigma_K)$. Because the sizes of both g_K and $G_m(\sigma_K)$ are reduced to $2^{-K}\times 2^{-K}$, the computation time is dramatically reduced. To avoid the loss of original image information, in this paper the minimum image size of the top level K image obtained by the down-sampling process is limited to 32×32.

Table I gives examples of the computation time before and after Gaussian pyramid for two different size images. For the original image g_0 with size of 256×192, the size of top image g_2 is reduced to 64×48 after $K=2$ steps down sampling. Because of $\sigma_m=\sigma_K\times 2^K$, in this case of $K=2$, we need to compute the convolutions for $\sigma_K=2,4,8,16,32$, equivalent to $\sigma_m=8,16,32,64,128$, respectively. For $\sigma_m=64$ and 128, before and after Gaussian pyramid the computation time is reduced to about 1/10 and 1/15, respectively. The time is further reduced with increasing σ_m. For larger image size, 1280×960, after $K=4$ steps down-sampling, the size of top image g_4 is reduced to 80×60. As Table I(b) illustrates, we need only to compute $\sigma_K=2,4,8$, equivalent to $\sigma_m=32,64,128$, respectively. The computation

Table I. Reduction in process time by Gaussian pyramid.

			Image size	
(a)	Scale		256×192 process time (s)	$256\times 192(64\times 48)$ process time (s)
	m	σ_m	Normal	Pyramid
	3	8	0.29	0.24
	4	16	0.75	0.24
	5	32	2.40	0.39
	6	64	9.13	0.90
	7	128	166.3	10.65
			Image size	
(b)	Scale		1280×960 process time (s)	$1280\times 960(80\times 60)$ process time (s)
	m	σ_m	Normal	Pyramid
	5	32	59.10	5.13
	6	64	236.1	5.34
	7	128	4118	9.29

time is reduced to about 1/10, 1/45, and 1/450 after the pyramid, respectively. The computation time is even more dramatically reduced not only with increasing σ_m, but also with increasing image size. As shown in Table I(b), for image size 1280×960, the computation time is reduced to 1/443 for $\sigma_m=128$ after pyramid.

Since Gaussian pyramid processing uses the coarsest down-sampled image version of the original image for computation of the surround image, whether the Retinex image quality is affected or not has to be re-estimated. Again we evaluated the color difference between the resultant images after Gaussian pyramid and the target visual image color block. As shown in Fig. 9, in the case of $M=3$ with $\sigma_m=(2,16,128)$, the smallest color difference $\Delta E^*_{ab}=8.54$ is obtained when gain A=0.65, $w(\sigma_m)=0.1,0.1,0.8$. As well, for the case of $M=2$ with $\sigma_m=(2,128)$ in Fig. 10, the smallest color difference $\Delta E^*_{ab}=8.5$ is obtained when gain $A=0.6$, $w(\sigma_m)=0.1,0.9$. We also tested $\sigma_m=(8,32,128)$ equivalent to $\sigma_K=(2,8,32)$ for the same condition as subsection Optimum Parameters. Figure 11 illustrates the results. We obtain almost the same color reproduction accuracies through Gaussian pyramid processing.

Figure 12 gives some examples before and after Gaussian pyramid with the same parameters. The resultant image with Gaussian pyramid is much the same as the results without Gaussian pyramid. As visually observed in Fig. 12(a) through (f), the three pairs of resultant images for [$A=0.5$, $w(\sigma_m)=1/3$, $\sigma_m=8,32,128$], [$A=0.6$, $w(\sigma_m)=0.1,0.1,0.8$, $\sigma_m=8,32,128$], and [$A=0.8$, $w(\sigma_m)=0.2,0.1,0.7$, $\sigma_m=8,32,128$] resulted in much the same image appearance with and without Gaussian pyramid, and bear comparison with NASA in (h). Because the true target image is unknown in this outdoor scene, the optimal parameters may be different from those of test target image color block. The proposed system resulted in the excellent rendition (i) even for the default parameters, $A=0.5$, $w(\sigma_1)=w(\sigma_2)=0.5$, $\sigma_m=2,128$ with Gaussian pyramid.

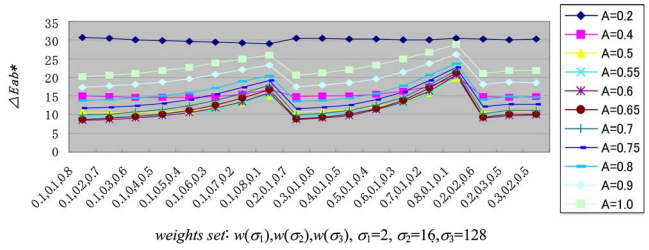

Figure 9. Color reproducibility by proposed pyramid with three-scale sets ($\sigma_m=2,16,128$).

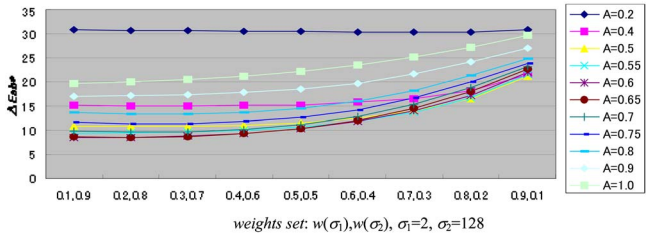

Figure 10. Color reproducibility by proposed pyramid with two-scale sets ($\sigma_m=2,128$).

HIGH DYNAMIC RANGE (HDR) IMAGE COMPRESSION

The proposed model also worked well for HDR image compression. Considering the computation time, we again adopted the pyramid process to create the surround image. We did not need any particular postprocess for normal LDR images after Retinex process to regulate the dynamic range. But for the most HDR images, a postprocess is necessary for displaying them onto normal LDR display devices. Here the luminance channel is also applied to compute the surround for our HDR image compression in order to maintain color balance. First, we compute the integrated surround Retinex image $Y_R(x,y)$ for HDR luminance channel by

$$Y_R(x,y)=\frac{Y(x,y)}{S_{\text{sum}}}. \tag{14}$$

Then we make use of Y_R to obtain the condition for compressing the HDR image to LDR image for the display device. We found that the histogram of Y_R is mostly concentrated in the lower range, while scattered in the middle to higher ranges for our tested HDR images as illustrated in Fig. 13. Thus we divided the higher range of Y_R by large interval and the lower range by small interval not to lose the details. First, the histogram of Y_R is divided into two parts [Min-Mean] and [Mean-Max] by the mean value Mean. Second, the pixel numbers Num_1 less than Mean and Num_2 larger than Mean are calculated respectively. Third, the ratios of Num_1 and Num_2 to all pixel numbers are calculated by Eqs. (15) and (16). Then, the bins are calculated by Eq. (17),

$$\text{ratio}_1=\frac{\text{Num}_1}{\text{Num}_1+\text{Num}_2}, \tag{15}$$

$$\text{ratio}_2=\frac{\text{Num}_2}{\text{Num}_1+\text{Num}_2}, \tag{16}$$

$$\text{bin}_1=255*\text{ratio}_1;\quad \text{bin}_2=255*\text{ratio}_2. \tag{17}$$

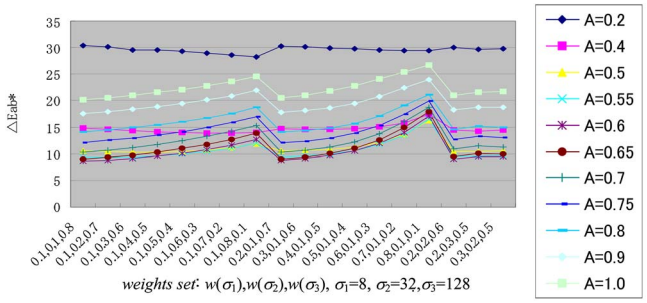

Figure 11. Color reproducibility by proposed pyramid with three-scale sets ($\sigma_m=8,32,128$).

Figure 12. Samples by the proposed model.

Then the two ranges of [Min-Mean] and [Mean-Max] are uniformly divided into bin_1 and bin_2 respectively. Accordingly, the Y_R image is divided into 255, which provides an image which can be displayed on normal display devices, expressed by $Y_d(x,y)$. Finally, the compressed color image $I_{di}(x,y)$ is reproduced by Eq. (18), where γ denotes a gamma correction coefficient. In this paper, $\gamma=0.5$ is used

$$I_{di}(x,y) = \left(\frac{I_i(x,y)}{Y(x,y)}\right)^{\gamma} Y_d(x,y). \tag{18}$$

Figures 14–17 show some experimental results. For the next part, the images in (a) by the proposed model are compared with those in (b) by Larson's histogram adjustment method.[27] In total, our results are much the same as Larson's results in spite of its simple and fast algorithm. However, unfortunately, our result in Fig. 14 looks worse than Larson's and different from other samples. It has a drawback that the water drops on the right side glass door are overenhanced thereby reducing its resolution. We have not found the cause of this phenomenon yet, but it may come from an improper choice of weights and kernel sizes to create the integrated surround. On the contrary, in Figs. 16 and 17, the proposed method could display some areas visibly which are invisible in Larson's results.[28]

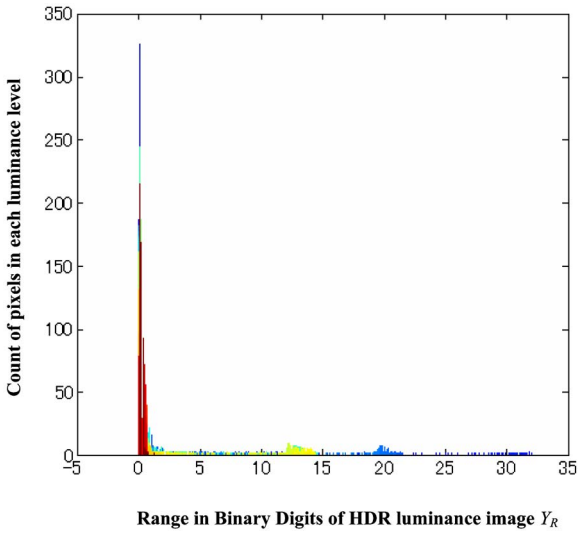

Figure 13. Histogram of luminance image by proposed Retinex of high dynamic range image.

CONCLUSIONS

In this paper, a concise and fast Retinex algorithm different from conventional MSR is proposed by integrating multiscale surround images into a single surround. The proposed model worked as well as MSR in suppressing the banding artifacts obtained by conventional SSR. In addition, the computation time was dramatically reduced by introducing the Gaussian pyramid. This simple model worked nicely in appearance improvement for both normal LDR and HDR images with range compression. Retinex has a goal to reproduce the original scene just as the observer may have seen it. To find the optimum parameters, we synthesized a target image on display visually matched to the real scene as observed by naked eye in the experimental room. A simple test target color block is captured under nonuniform illumination in the experimental room and used for evaluating the color reproducibility. Finding more robust and stable pa-

Figure 14. Bathroom: (a) by proposed model and (b) by Larson with histogram adjustment.

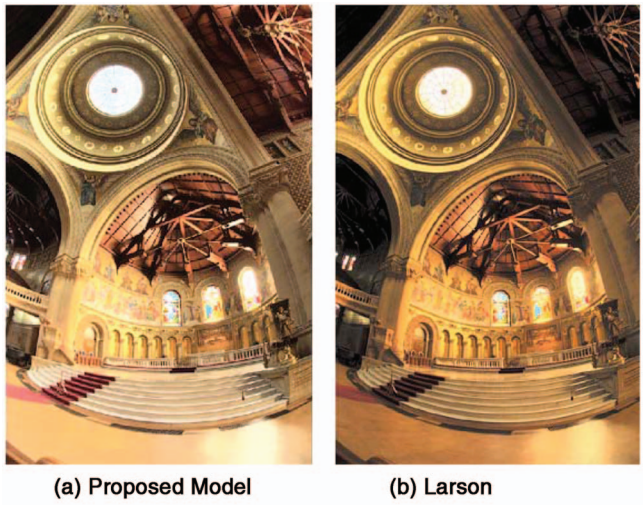

Figure 15. Memorial Church: (a) by proposed model and (b) by Larson with histogram adjustment.

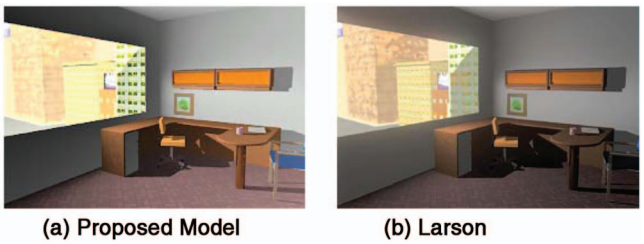

Figure 16. Win office: (a) by proposed model and (b) by Larson with histogram adjustment.

rameters in a full automatic mode for more complicated target images is left to future work involving psychophysical tests.

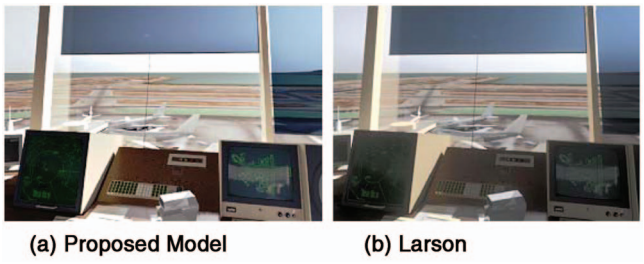

Figure 17. Air traffic tower: (a) by proposed model and (b) by Larson with histogram adjustment.

ACKNOWLEDGMENT

The authors would like to thank Ward Larson for his help with the HDR images used in this paper.

REFERENCES

[1] J. DiCarlo and B. Wandell, "Rendering high dynamic range images", Proc. SPIE **3956**, 392 (2001).
[2] J. Tumblin, J. Hodgins, and B. Guenter, "Two methods for display of high contrast images", ACM Trans. Graphics **18**, 56 (1999).
[3] J. Tumblin and H. Rushmeier, "Tone reproduction for realistic images", IEEE Comput. Graphics Appl. **13**, 42 (1993).
[4] S. N. Pattanaik, J. Tumblin, H. Yee, and D. P. Greenberg, "Time-dependent visual adaptation for fast realistic image display", *Proc. SIGGRAPH* (ACM/Addison-Wesley, New York, 2000) pp. 47–54.
[5] K. Chiu, M. Herf, P. Shirley, S. Swamy, C. Wang, and K. Zimmerman, "Spatially nonuniform scaling functions for high contrast images", *Proceedings of Graphics Interface 93* (Morgan Kaufmann, San Francisco, CA, 1993) pp. 245–253.
[6] H. Kotera and M. Fujita, "Appearance improvement of color image by adaptive scale-gain Retinex model", *Proc. IS&T/SID 10th Color Imaging Conference* (IS&T, Springfield, VA, 2002) pp. 166–171.
[7] Y. Yoda and H. Kotera, "Appearance improvement of color image by adaptive linear Retinex model", *Proc. IS&T's NIP21* (IS&T, Springfield, VA, 2004) pp. 660–663.
[8] S. Carrato, "A pseudo-Retinex approach for the visualisation of high dynamic range images", *Proc. 5th COST 276 Workshop* (COST, European Science Foundation, Brussels, 2003) pp. 15–20.
[9] E. H. Land, "The Retinex", Am. Sci. **52**, 247 (1964).
[10] E. H. Land and J. J. McCann, "Lightness and the Retinex theory", J. Opt. Soc. Am. **61**, 1 (1971).
[11] E. H. Land, "The Retinex theory of colour vision", Proc. R. Institution Gr. Britain **47**, 23 (1974).
[12] E. H. Land, "Recent advances in the Retinex theory and some implications for cortical computations: Color vision and the natural image", Proc. Natl. Acad. Sci. U.S.A. **80**, 5163 (1983).
[13] E. H. Land, "An alternative technique for the computation of the designator in the Retinex theory of color vision", Proc. Natl. Acad. Sci. U.S.A. **83**, 3078 (1986).
[14] J. Frankle and J. J. McCann, "Method and apparatus for lightness imaging", US Patent 4,384,336 (1983).
[15] R. Kimmel, "A variational framework for Retinex", Int. J. Comput. Vis. **52**, 7 (2003).
[16] J. J. McCann, "Lessons learned from Mondrians applied to real images and color gamuts", *Proc. IS&T/SID 7th Color Imaging Conference* (IS&T, Springfield, VA, 1999) pp. 1–8.
[17] J. J. McCann, "Retinex at 40", J. Electron. Imaging **1**, 6 (2004).
[18] B. Funt, V. Cardei, and K. Barnard, "Learning colour constancy", *Proc. IS&T/SID 4th Color Imaging Conference* (IS&T, Springfield, VA, 1996) pp. 58–60.
[19] A. Blake, "Boundary conditions of lightness computation in Mondrian world", Comput. Vis. Graph. Image Process. **32**, 314 (1985).
[20] J. J. McCann and I. Sobel, "Experiments with Retinex", HPL Color Summit (Hewlett Packard Laboratories, Technical Report, 1998).
[21] B. Funt, F. Ciurea, and J. McCann, "Retinex in MATLAB", *Proc. IS&T/SID 8th Color Imaging Conference* (IS&T, Springfield, VA, 2000) pp. 112–121.
[22] Z. Rahman, "Properties of a center/surround Retinex: Part 1: Signal processing design", NASA Contractor Report 198194 (1995), p. 13.

[23] D. J. Jobson and G. A. Woodell, "Properties of a center/surround Retinex: Part 2: Surround design", NASA Technical Memorandum 110188 (1995), p. 15.
[24] Z. Rahman, D. J. Jobson, and G. A. Woodell, "Multiscale Retinex for color rendition and dynamic range compression", Proc. SPIE **2847**, 183 (1996).
[25] D. J. Jobson, Z. Rahman, and G. A. Woodell, "Properties and performance of the center/surround Retinex", IEEE Trans. Image Process. **6**, 451 (1997).
[26] Z. Rahman, D. J. Jobson, and G. A. Woodell, "Retinex processing for automatic image enhancement", Proc. SPIE **4662**, 390 (2002).
[27] W. Larson, H. Rushmeier, and C. Piatko, "A visibility matching tone reproduction operator for high dynamic range scenes", IEEE Trans. Vis. Comput. Graph. **3**, 291 (1997).
[28] http://www.truview.com/images.